Stromal Antiapoptotic Paracrine Loop in Perineural Invasion of Prostatic Carcinoma

Gustavo E. Ayala,[1,2] Hong Dai,[1] Salahaldin A. Tahir,[2] Rile Li,[1] Terry Timme,[2,3] Michael Ittmann,[1] Anna Frolov,[2] Thomas M. Wheeler,[1,2] David Rowley,[3] and Timothy C. Thompson[2,3]

Departments of [1]Pathology, [2]Urology, and [3]Molecular and Cellular Biology, Baylor College of Medicine, Houston, Texas

Abstract

Caveolin-1 (cav-1) is a major scaffolding component of cell membrane invaginations (caveolae). It is involved in sequestering numerous effectors and signaling molecules and has antiapototic activities in prostate cancer. Perineural invasion (PNI) is associated with decreased apoptosis of cancer cells both in human tissues and the *in vitro* PNI model. We show here that stromal (perineurium) production of cav-1 is involved in a paracrine antiapoptotic loop in PNI. Transforming growth factor-β1 is up-regulated in the cancer cells as they approach the nerve and is thought to up-regulate cav-1 in the perineurium of nerves with prostate cancer. Cav-1 is then secreted into the microenvironment and used by prostate cancer cells to inhibit apoptosis. In the *in vitro* PNI model, this phenomenon is partially reversed by neutralizing cav-1 antibodies or using ganglia from *cav-1* knockout mice. Our results show a novel paracrine mechanism used by the prostate cancer in PNI to increase their proliferative activity and decrease apoptosis. (Cancer Res 2006; 66(10): 5159-64)

Introduction

Perineural invasion (PNI) is a major contributor to extraprostatic spread of prostate cancer. However, the biology of PNI is poorly understood. In previous publications, we presented an *in vitro* model that reproduces PNI and used the model to show that symbiotic interactions between cancer and nerves result in costimulation of growth (1). Prostate cancer cells use PNI as a route for dissemination and also acquire a survival advantage during the process (2).

Our previous studies showed a survival advantage for prostate cancer cells in the perineural space manifested by reduced apoptotic activities and increased proliferation compared with prostate cancer cells in non-PNI sites (3). The *in vitro* PNI model reproduces this survival advantage when prostate cancer cells were cocultured with dorsal root ganglion (DRG) nerve tissue.

Caveolin-1 (cav-1) is a major scaffolding component of cell membrane invaginations, called caveolae, present in many different types of cells, including prostate cancer cells. It is involved in sequestering numerous effectors and signaling molecules (G-protein, calcium, mitogen-activated protein kinase, and lipid signaling components) and may facilitate their activities (4). Cav-1 also shows antiapoptotic activities in prostate cancer and has been associated with metastasis and androgen insensitivity in this malignancy (5). Although epithelial cav-1 expression correlates with pathologic variables associated with poor prognosis, it is an independent predictor of prostate-specific antigen recurrence after radical prostatectomy (6). Interestingly, cav-1 levels are higher in prostate cancers from African-American men compared with White-American men (7).

Cav-1 is also found in neural PC12 cells and DRG neurons (8). It is seen along the entire surface of DRG neurons, in Schwann cells, and in particularly high levels in growth cones (8). Cav-1 has also been associated with adhesion. A urokinase-type plasminogen activated receptor–integrin–cav-1 complex has been identified in prostate cancer cells and has been linked to adhesion sites (9). The presence of cav-1 on the contact surfaces of DRG and Schwann cells raises the possibility of cell-to-cell– or cell-to-matrix–initiated, cav-1/caveolae–mediated cell signaling that could trigger antiapoptotic effects. Because cav-1 is up-regulated in response to neuron injury (8), it is possible that nerves secrete cav-1 during PNI as a response to damage produced by the cancer cells to the nerve. To test if cav-1 is involved in the survival advantage found in cells in perineural location, we used the *in vitro* PNI model and tissue microarray technology.

Materials and Methods

***In vitro* PNI system.** The *in vitro* PNI coculture model consists of human prostate cancer cells (DU145) and mouse ganglia/nerves embedded in Matrigel following conditions we have published previously (1). Briefly, DRG/nerves from 4- to 7-week-old C57BL/6 mice were removed surgically and cocultured with DU145 cells in EHS Matrigel (Becton Dickinson, Bedford, MA). Cultures were grown in RPMI 1640 (Life Technologies, Grand Island, NY) containing 10% heat-inactivated fetal bovine serum (FBS, Life Technologies) in a humidified atmosphere of 5% CO_2. DU145 alone and DRG alone were cultured as controls. Between days 9 and 11, some cultures were fixed (3.7% buffered formalin) and processed for immunohistochemistry. Residual conditioned medium (48 hours) from all cultures were frozen for use in the microchamber system.

DRG from *cav-1* knockout mice and littermate wild-type controls were also used for a different set of experiments. These genetically engineered mice were described previously (10).

Microchamber system. DU145 human prostate carcinoma cells were obtained from American Type Culture Collection (Rockville, MD) and were cultured in RPMI 1640 supplemented with FBS (10%), penicillin (100 units/mL), and streptomycin (100 μg/mL; Sigma Chemical Company, St. Louis, MO). They were maintained at 37°C in a humidified atmosphere of 5% CO_2. DU145 cells were cultured in microchamber culture slides (VWR) as monolayer adherent cells for 11 days to ~70% to 80% confluency. The cultures were then switched to 50% fresh medium and 50% conditioned medium transferred from the PNI coculture model and controls (DU145 cell growing alone). Fresh RPMI-based culture medium was also used as a control. Recombinant human transforming growth factor-β1 latency-associated peptide (TGF-β1 LAP; R&D Systems, Minneapolis, MN), cav-1 neutralizing antibody (Santa Cruz Biotechnology, Santa Cruz, CA) or the normal goat IgG control (AB-108-C, R&D Systems) was added to the 100 μL cold growth factor reduced Matrix Matrigel (Becton Dickinson) separately. The Matrigel and antibody mixture was transferred by a prechilled pipette

Requests for reprints: Gustavo E. Ayala, Department of Pathology, Baylor College of Medicine, One Baylor Plaza, Houston, TX 77030. Phone: 713-798-3705; Fax: 713-798-2720; E-mail: gayala@bcm.tmc.edu.

©2006 American Association for Cancer Research.

doi:10.1158/0008-5472.CAN-05-1847

Downloaded from http://aacrjournals.org/cancerres/article-pdf/66/10/5159/2550770/5159.pdf by guest on 11 February 2025

tip into each well of a prechilled six-well plate. Then, 10^5 cells were seeded on 100 μL cold Matrigel around a mouse DRG. The amount of recombinant human LAP TGF-β1 added was based on the neutralization dose 50 (ND_{50}) for each. LAP was added per 100 μL Matrigel, which is 2.65× the ND_{50}. Dialyzed cav-1 neutralizing antibody (Santa Cruz Biotechnology) was added as 1:100, 0.2 μg per 100 μL Matrigel. As a control, an equivalent amount of normal goat IgG (R&D Systems) was added. For all conditions, DU145/DRG *in vitro* model were allowed to develop for 12 days in RPMI 1640 containing 5% Nu serum (BD Biosciences, Bedford, MA) in a humidified atmosphere of 5% CO_2. An equivalent concentration of each antibody was added into culture medium, respectively. After washing by 1× D-PBS, samples were harvested from six-well plate, then mixed with 4% agar, chilled on ice, and transferred to tissue cassette. Samples were fixed in 10% neutralized formalin overnight at room temperature. Then, embedded in paraffin, 5 μm sections were cut and mounted onto slides.

First-strand cDNA synthesis. First-strand cDNA was made from total RNA by using RETROscript First Strand Synthesis kit (Ambion, Austin, TX). One microgram of each RNA sample and control template RNA (Ambion) was heated to 75°C for 3 minutes in nuclease-free water containing 2 μL random decamers. Reverse transcriptase buffer (10×, 2 μL), 4 μL of 10 mmol/L deoxynucleotide triphosphate mix (dATP, dCTP, dGTP, and dTTP, 10 mmol/L each), 1 μL placental RNase inhibitor, and 1 μL Moloney murine leukemia virus reverse transcriptase (100 units/μL) were added to the sample. Each reaction volume was adjusted to 20 μL by adding nuclease-free water. The reaction mixture was incubated at 44°C for 1 hour, followed by incubation at 92°C for 10 minutes to inactivate the reverse transcriptase.

Real-time quantitative PCR. The ABI Prism 7000 sequence detection system (Applied Biosystems, Foster City, CA) was used for quantitative PCR analysis using hypoxanthine phosphoribosyltransferase 1 (HPRT1) as endogenous control. All probes (6-FAM dye labeled at the 5′ end and a nonfluorescent quencher at 3′ end of the probe) were combined with primers (Assay-on-Demand, Hs 00171257_m1; Hs 99999909_m1; Applied Biosystems). Validation experiments were done using 1:2 diluted total RNA templates. The log input amount of RNA versus change in cycle threshold (ΔC_t) was generated to show that the efficiencies of the targets and references were approximately equal. TGF-β1 and HPRT1 were amplified in separate wells in duplicate. Reaction conditions included 10 μL of 2× Taqman Universal Master Mix (with UNG), 1 μL HPRT1 or TGF-β1 primers and probes mixture, 100 ng template cDNA (DU145 alone and PNI coculture), and nuclease-free water to a 96-well reaction plate. The Taqman cycling conditions were as follows: 2 minutes at 50°C, 10 minutes at 95°C, and 40 cycles of 15 seconds at 95°C followed by 1 minute at 60°C.

The calculation was done using values of ΔC_t as the calibrator from DU145 cells cultured alone or from DU145 cells cocultured with DRG. For each experimental sample, the C_t of target, normalized to an endogenous reference and relative to a calibrator, is given by: $2 - \Delta^{\Delta C_t}$.

Tissue microarray. Tissue microarrays were built using tissues from 50 human prostate cancer patients treated by radical prostatectomy at Baylor College of Medicine–affiliated hospitals using the manual tissue arrayer (Beecher Instruments Microarray Technology, Silver Spring, MD). Tissues from these patients were processed following standard procedures. Whole-mount slides were examined under light microscope and areas of nerves with PNI as well as areas of cancer as far away as possible from the nerve were selected and cored (one tissue cylinder, 2 mm).

***In situ* labeling of apoptotic bodies.** The detection of DNA fragmentation was determined *in situ* by the terminal deoxynucleotidyl transferase–mediated dUTP biotin nick end labeling (TUNEL) technique as described previously (11). We used the TACS·XL-DAB *in situ* apoptosis kit (Trevigen, Inc., Gaithersburg, MD) following the instructions of the manufacturer with minor modifications, and counterstained with methyl green. The TUNEL assay and immunohistochemistry were done on the tissue microarray slides and paraffin-embedded sections of PNI coculture and controls. A positive control slide prepared by TACS-nuclease and a specimen known to be positive for apoptotic cells were used as positive controls. Substitution of terminal deoxynucleotidyl transferase enzyme with distilled water was used as a negative control.

Apoptotic bodies were counted under a light microscope (×400) equipped with an ocular grid (10,000 μm^2). The area with highest positive stain was selected for counting. The number of apoptotic bodies was determined in a total of ~2,000 prostate cancer cells, normalized to 100 cells, and defined as apoptotic index. At least 10 representative areas without necrosis were selected. Positively staining cells or bodies located in the stroma and lumen were excluded because these apoptotic cells or bodies might have originated from other cell types.

Western blotting. To test if secreted cav-1 was present in our cocultures, we used Western blots with antibodies against cav-1 (polyclonal cav-1 antibody, Santa Cruz Biotechnology) in the supernatant obtained from the *in vitro* cocultures (DRG/DU145) and the controls (DU145 alone and DRG alone) using methodology described previously (4).

Immunoperoxidase. Expression of cav-1 and TGF-β1 protein in histologic sections was analyzed by immunohistochemistry. The following primary antibodies were used: polyclonal anti-cav-1 antibody (polyclonal IgG, 1;10 dilution, 30-minute incubation time; Santa Cruz Biotechnology) and TGF-β1 (polyclonal IgG, 1;10 dilution, 30-minute incubation time; Santa Cruz Biotechnology). The secondary biotinylated antibody was applied for 30 minutes followed by 30 minutes of incubation with streptavidin peroxidase (LSAB + HRP kit; DAKO). After rinsing, slides were visualized by diaminobenzidine chromogen solution (DAKO, Philadelphia, PA) and counterstained with routine hematoxylin.

Assessment of immunostaining. All stained slides were digitized using an automated slide scanner (Bacus Laboratories, Lombard, IL) to produce an image of every dot and also inform the dot coordinates on the slide. Each image was interpreted for immunoreactivity using a 0 to 3+ semiquantitation scoring system for both the intensity of stain and percentage of positive cells (percentage labeling frequency). For the intensity, the grading scale ranged from no detectable signal (0) to strong signal seen at low power (3). A moderate signal seen at low to intermediate power was designated 2, whereas 1 indicated a weak signal seen only at intermediate to high power. Labeling frequency was scored as 0 (0%), 1 (1-33%), 2 (34-66%), or 3 (67-100%). The multiplicative index of intensity and labeling was considered for analysis in the case of TGF-β1. The multiplicative index was obtained by totaling the scores of intensity and percentage (i.e., if the intensity score was 3 and the labeling index 2, the multiplicative index is 6). For cav-1 expression analysis, we used only the intensity of stain.

Positive staining of Ki-67 was confined to the nucleus. The proliferation index was defined as the ratio of KI-67-positive cancer cells to total cancer cells in the highest positive stain fields (at least 2,000 cells in multiple fields), using a microscopic grid at ×400 magnification. In the cav-1 knockout experiment, we compared the proliferative indices from days 2 and 5. We divided the former by the latter to obtain the rate of change in the proliferation index.

Statistical analysis. Comparisons between indices of proliferation and apoptosis were done using Mann-Whitney nonparametric tests. Logistic regression was used to account for interexperimental variability for these comparisons. $P < 0.05$ were considered statistically significant. All analyses were done using the SPSS 12.0 software package (SPSS, Inc., Chicago, IL).

Results

Cav-1 expression is increased in human perineural cells of nerves with PNI. While examining prostate specimens stained for cav-1, we identified cav-1 expression by perineural cells. To test if cav-1 expression changed during PNI, we used tissue microarrays. Cav-1 expression by the perineural cells was increased in nerves with PNI (mean, 1.85; median, 2; $n = 40$) compared with nerves spatially unrelated to prostate cancer (mean 1.17, median 1, $n = 54$; $P < 0.0001$). From the 50 patients in this array, we identified 18 that, within the same 2 mm dot, had nerves with and without prostate cancer PNI concomitantly. Cav-1 expression within the perineurium was increased in 16 of 18 cases (Fig. 1*C*). We did not identify cav-1 in the perineural prostate cancer cells (Fig. 1*A* and *B*). This is

Downloaded from http://aacrjournals.org/cancerres/article-pdf/66/10/5159/2550770/5159.pdf by guest on 11 February 2025

A

Perineural Caveolin	Nerve Alone	Nerve w/ Perineural Invasion
Upregulation	1	16
Downregulation	-	1
No change	1	1

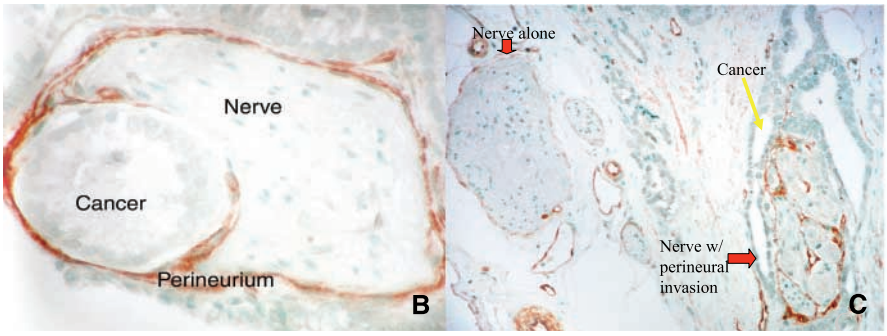

Figure 1. *A,* matched pair analysis of nerves with PNI and nerves without PNI of the same patient show that most of the former have up-regulation of cav-1 in their perineurium. Although 16 cases had up-regulation, only one had similar levels and one had decreased levels of caveolin in the perineurium. *B,* immunohistochemical detection of cav-1 in the perienurium of prostatic nerves in human tissue microarray specimens *C,* a nerve without prostate cancer with weak expression of cav-1 (*left*). Cav-1 expression in the perineurium increases in the nerve with perineral invasion (*right*). Both are human tissue microarray specimens.

most likely due to the sampling error because cav-1 expression by cancer cells is patchy.

Cav-1 is secreted into the supernatant of the *in vitro* PNI model. We were able to identify secreted cav-1 in the supernatant originating from the DRG/DU145 model only on day 13 (Fig. 2). It is of note that this is the time when perineural halo formation is seen in the *in vitro* system. This result matches the observation in human prostate cancer, where cav-1 expression is increased when PNI is present.

Cav-1 antibody reduces the survival activities contained in the supernatant from the *in vitro* PNI model. The supernatant from the DU145 + DRG coculture also induced a decrease in apoptosis in the cocultured cells. There was a marked decrease in the mean apoptotic index in the cells cultured with the supernatant from the coculture (3.2 ± 1.52, $n = 25$) compared with that in the cells with the supernatant from the DU145 cells growing alone (5.47 ± 1.76, $n = 20$; $P < 0.0001$). Antibodies against cav-1 partially reversed the inhibition of apoptosis in the cells cultured with supernatant from the cocultures (medians: 0.20 versus 1.85; $P = 0.0253$), whereas IgG had no effect on the apoptotic rate (0.33, $P = 0.5926$; Fig. 3*B*). Neutralizing cav-1 antibodies also decreased the proliferation index compared with the PNI coculture (medians: 75.0 versus 17.5; $P = 0.0253$), whereas IgG had no effect (59.8; $P = 0.4795$).

***Cav-1* knockout nerves have reduced prosurvival activities.** The PNI *in vitro* model was run using DRG from *cav-1* knockout mice and compared with the wild-type litter controls. The supernatant from both conditions was analyzed by Western blotting to detect the presence of cav-1. Cav-1 was reduced ~50% in the *cav-1* knockout–derived supernatant compared with wild-type control supernatant (151 versus 93). It is well known that prostate cancer cells produce cav-1, and it is most likely that the residual cav-1 present in the supernatant comes form the cancer cells. More importantly, we identified a decrease in the rate of change in the proliferation index from day 2 to 5 in the *cav-1* knockout PNI model cells compared with those in the controls. The decrease in proliferative index was significant after adjustment for interexperiment variability (D + N: mean = 0.2555, median = 0.2370/ D + N-cav: mean = 0.1892, median = 0.2072; $P = 0.0393$; Fig. 4).

TGF-β1 is increased in cancer cells in the perineural location. Previous studies have shown that cav-1 secretion is influenced by numerous growth factors, most notably TGF-β1. To test a correlation between cav-1 and TGF-β1 in cells in PNI, we used quantitative reverse transcription-PCR (RT-PCR) and immunohistochemistry. By quantitative RT-PCR, we showed over twice the levels of TGF-β1 total RNA in cancer cells from the DU145/DRG coculture compared with DU145 cells growing alone (Fig. 5*A*). This finding was corroborated at the protein level in human tissues using immunohistochemistry. TGF-β1 expression by the perineural cells was increased in nerves with PNI (mean 4.32, median 2, $n = 38$) compared with nerves spatially unrelated to prostate cancer (mean 2.87, median 1, $n = 38$; $P = 0.0002$). We also identified a gradient of prostate cancer cytoplasmic expression, with cancer approaching the nerve expressing TGF-β1 more intensely (Fig. 5*B* and *C*). TGF-β1 was also found expressed in the DU145 cells in the *in vitro* model.

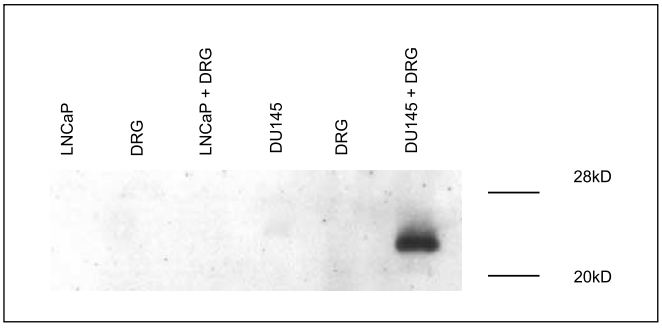

Figure 2. Western blot with antibodies against cav-1 reveal secreted caveolin detection in the supernatant of DU-145 + DRG coculture on day 13. We did not detect cav-1 in the supernatant of LnCap, DRG, or LnCap + DRG cocultures on that day.

Downloaded from http://aacrjournals.org/cancerres/article-pdf/66/10/5159/2550770/5159.pdf by guest on 11 February 2025

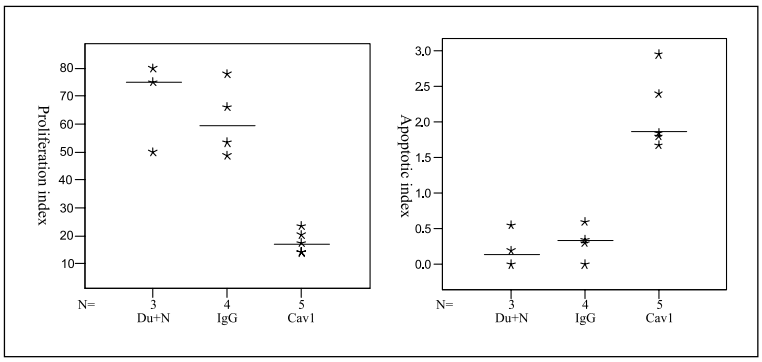

Figure 3. *Left,* decrease in the proliferation rate in the PNI when cav-1-neutralizing antibodies are added to the model. The addition of IgG has no effect on the process. *Right,* increase in apoptosis with neutralizing antibodies to cav-1 in the supernatant, whereas IgG has no effect. *N,* number of experiments. *, average for an individual experiment; *bar,* median of all experiments.

Furthermore, addition of LAP to the PNI coculture increased the apoptotic rate (medians: 0.20 versus 1.40; $P = 0.0495$; Fig. 5*E*) and decreased the proliferation rate (75.0 versus 34.5; $P = 0.0495$; Fig. 5*D*), confirming a partial reversal of function by inhibition of the TGF-β1 axis.

Discussion

Consideration of the tumor microenvironment is critical in understanding cancer progression. We have shown previously that the tumor microenvironment can have significant effects on the survival and progression of prostate cancer (2, 3). In this report, we show that PNI in prostate cancer is associated with a decrease in apoptosis *in vitro* and in human tissues. We also show that this process is regulated at least in part by secreted substances. Importantly, we define a prosurvival regulatory pathway that is dependent on perineural stromal cell–derived secreted cav-1. Our results have implications for the development of prognostic/predictive biomarkers for prostate cancer and reveal new therapeutic targets for this malignancy.

All carcinomas have two major components; the epithelium, which is regarded as the malignant element and the supporting stroma, which we regard as a reactive and regulatory element. We have previously shown that the stroma in the prostate responds to cancer development with a generic type of a wound repair type process (12, 13). Available evidence suggests that initial carcinoma growth is stromal dependent, where the stroma is permissive and supporting, and is regulated through paracrine interactions with the carcinoma cells (12, 14). However, the influence of stromal elements, other than the myofibroblast, has been understudied in cancer research. Vessels and nerves have been considered targets for cancer involvement, and not active participants in the progression of disease. The supporting function of the perineurium and nerves has not been adequately addressed.

The *in vitro* PNI model has enabled us to study mechanisms that might be related to the inhibition of apoptosis in the perineural space as it reproduces PNI with great fidelity (1). We presume that the perineural space is a favorable microenvironment that plays a critical role in nerve-epithelial interactions to facilitate prostate cancer growth and PNI. The nerves not only give cancer a route through which to spread, but also provides a microenvironment that is advantageous for growth through inhibition of apoptosis and increased proliferation (1–3). Previously, we showed that the increase in proliferation and the decrease in apoptosis are regulated, in part, through the nuclear factor-κB (NF-κB) pathway and it downstream effectors Pim-2 and defender against death (3). We do not consider the activation of multiple antiapoptotic pathways (i.e., the cav-1 pathway and the NF-κB pathway) in prostate cancer to be unusual. In fact, it is common to have redundant mechanisms that promote malignant progression. The NF-κB pathway is an intrinsic epithelial pathway, whereas the currently described cav-1 pathway involves stromal-epithelial interactions.

Cav-1 is expressed predominantly by the stroma, but is also overexpressed in a proportion of prostate cancer cases. It was also associated with increased viability of prostate cancer cell lines and adverse prognosis in patients (15). Cav-1 has also been found in neurons and nerves (8). Caveolae-like domains purified from

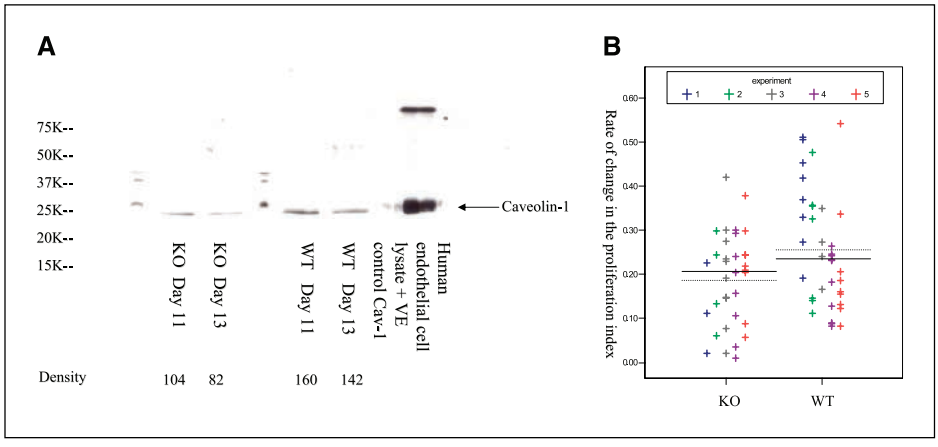

Figure 4. *A,* Western blot with antibodies against cav-1. Note the decrease in caveolin in the far left lanes, corresponding to the experiments with ganglia from cav-1 knockout, compared with the wild-type caveolin ganglia experiments. Note that the positive control lane is separated by an empty lane from the WT Day 13 lane. Densitometry readings are underneath. *B,* decrease in the rate of change in the proliferation index from day 2 to 5 in prostate cancer cells (Du-145) using ganglia from cav-1 knockout (*KO*), compared with the wild-type caveolin ganglia experiments (*WT*). +, individual reading per field from one experiment. The experiments are color-coded.

Downloaded from http://aacrjournals.org/cancerres/article-pdf/66/10/5159/2550770/5159.pdf by guest on 11 February 2025

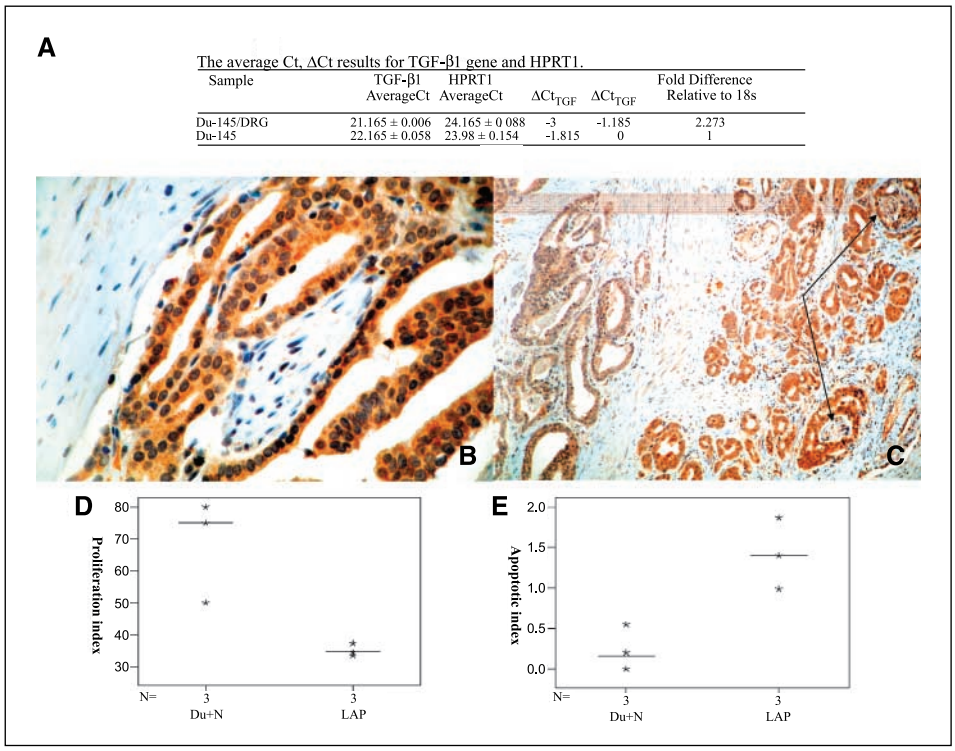

Figure 5. *A,* quantitative PCR results denoting an increase in TGF-β1 RNA levels in the DU-145 + nerve cocultures compared with controls. *B* and *C,* immunohistochemical detection of TGF-β1 in the cancer cells in perineural location in human tissues. Note the gradient of expression in *C* (*bar on top*). *Left,* prostate cancer away from the nerve has lower levels of TGF-β1 expression, whereas cancer spatially related to the nerves has higher levels of TGF-β1 (*right; arrows,* nerves). *D* and *E,* addition of LAP to the supernatant of the PNI coculture induces a partial reversal of the inhibition of apoptosis and increase in proliferation. Addition of LAP produces a decrease in proliferation (*left*) and an increase in apoptosis (*right*) compared with the Du + N controls. *N,* number of experiments; *, average for an individual experiment; *bar,* median of all experiments.

neuronal plasma cell membranes contain receptor tyrosine kinases, including insulin and neurotrophin receptors, Trk-B, and p-75 nerve growth factor receptors (16, 17). Direct interactions between cav-1 and neurotrophin receptors, such as Trk-A, Trk-B, and p75, may have functional consequences in the regulation of different pathways including those related to apoptosis (18). It is important to note that p75 is a negative regulator of prostate cancer growth through induction of apoptosis (19).

Our studies have shown that cav-1 is expressed by the perineurium of nerves in the prostate. This expression is increased significantly in the presence of PNI. Whether this increased expression is due to nerve injury caused by tumor infiltration remains to be established. Importantly, cav-1 was detected in conditioned medium from androgen-insensitive mouse and human prostate cancer cells (DU145, PC3, and TSU-Pr1) in variable amounts. Cav-1 was also expressed in high-passage LNCaP cells and secreted into the medium, but not expressed in low-passage LNCaP cells. In contrast, nonprostatic cells, such as endothelial, fibroblast, and smooth muscle, had a substantial amount of intracellular cav-1, yet minimal or nondetectable levels of cav-1 in their conditioned medium (4). We have shown that cav-1 is increased in the perineurium and also secreted into the microenvironment in the late stages of PNI. It is important to note that we only identified cav-1 in the coculture supernatant starting on day 11, when full contact between cancer cells and nerves had been established, although there has been some biological variability in the process. The supernatant experiment data indicates that secreted factors are responsible, at least in part, for the survival advantage shown by cells in the perineurium.

Invasion produces injury and wound response. It is conceivable that nerve injury produced by the invasive cancer cells is responsible for the increased expression and subsequent secretion of cav-1 into the perineural microenvironment as part of the wound-repair process. The mechanisms responsible for induction of cav-1 expression within the perineurium are unclear at this time. However, the reduction of function observed with the neutralizing cav-1 antibodies and the reduction in proliferative index when using ganglia from *cav-1* knockout mice in the *in vitro* PNI model indicate that secreted cav-1 is involved in the regulation of growth in the perineural space.

An interactive process, such as PNI, requires integrated signaling and regulatory systems. Our previous and current findings lead us to suggest that cancer cells send signals to nerves and/or perineurium to stimulate the production of antiapoptotic substance(s), which, in turn, facilitates the growth of cancer cells and induces them to migrate along nerve trunks. When prostate cancer invades the nerve in PNI, bioactive TGF-β1 is overexpressed by the cancer cells, as shown by the human tissue and *in vitro* PNI model studies, including the functional LAP experiment. We propose that cancer cell–derived TGF-β1, potentially in combination with a local wound response related to nerve injury, in turn, up-regulates cav-1 in the perineural cells, which is then secreted into the perineural microenvironment. Through this paracrine loop, secreted cav-1 can be used by the cancer cells to increase survival through down-regulation of apoptotic activities and increased proliferation. In our view, these microenvironment-driven activities are critical determinants of the increased malignant potential of prostate cancer that results from PNI.

Acknowledgments

Received 5/26/2005; revised 2/22/2006; accepted 3/10/2006.

Grant support: NIH Specialized Programs of Research Excellence grant CA58204 and Department of Defense grant PC 991371.

The costs of publication of this article were defrayed in part by the payment of page charges. This article must therefore be hereby marked *advertisement* in accordance with 18 U.S.C. Section 1734 solely to indicate this fact.

Downloaded from http://aacrjournals.org/cancerres/article-pdf/66/10/5159/2550770/5159.pdf by guest on 11 February 2025

References

1. Ayala GE, Wheeler TM, Shine HD, et al. *In vitro* dorsal root ganglia and human prostate cell line interaction: redefining perineural invasion in prostate cancer. Prostate 2001;49:213–23.
2. Yang G, Wheeler TM, Kattan MW, Scardino PT, Thompson TC. Perineural invasion of prostate carcinoma cells is associated with reduced apoptotic index. Cancer 1996;78:1267–71.
3. Ayala GE, Dai H, Ittmann M, et al. Growth and survival mechanisms associated with perineural invasion in prostate cancer. Cancer Res 2004;64:6082–90.
4. Tahir SA, Yang G, Ebara S, et al. Secreted caveolin-1 stimulates cell survival/clonal growth and contributes to metastasis in androgen-insensitive prostate cancer. Cancer Res 2001;61:3882–5.
5. Li L, Yang G, Ebara S, et al. Caveolin-1 mediates testosterone-stimulated survival/clonal growth and promotes metastatic activities in prostate cancer cells. Cancer Res 2001;61:4386–92.
6. Yang G, Truong LD, Wheeler TM, Thompson TC. Caveolin-1 expression in clinically confined human prostate cancer: a novel prognostic marker. Cancer Res 1999;59:5719–23.
7. Yang G, Addai J, Ittmann M, Wheeler TM, Thompson TC. Elevated caveolin-1 levels in African-American versus White-American prostate cancer. Clin Cancer Res 2000;6:3430–3.
8. Galbiati F, Volonte D, Gil O, et al. Expression of caveolin-1 and -2 in differentiating PC12 cells and dorsal root ganglion neurons: caveolin-2 is up-regulated in response to cell injury. Proc Natl Acad Sci U S A 1998;95:10257–62.
9. Wei Y, Yang X, Liu Q, Wilkins JA, Chapman HA. A role for caveolin and the urokinase receptor in integrin-mediated adhesion and signaling. J Cell Biol 1999;144:1285–94.
10. Cao G, Yang G, Timme TL, et al. Disruption of the caveolin-1 gene impairs renal calcium reabsorption and leads to hypercalciuria and urolithiasis. Am J Pathol 2003;162:1241–8.
11. Gavrieli Y, Sherman Y, Ben-Sasson SA. Identification of programmed cell death *in situ* via specific labeling of nuclear DNA fragmentation. J Cell Biol 1992;119:493–501.
12. Tuxhorn JA, Ayala GE, Rowley DR. Reactive stroma in prostate cancer progression. J Urol 2001;166:2472–83.
13. Tuxhorn JA, Ayala GE, Smith MJ, Smith VC, Dang TD, Rowley DR. Reactive stroma in human prostate cancer: induction of myofibroblast phenotype and extracellular matrix remodeling. Clin Cancer Res 2002;8:2912–23.
14. Rowley DR. What might a stromal response mean to prostate cancer progression? Cancer Metastasis Rev 1998;17:411–9.
15. Satoh T, Yang G, Egawa S, et al. Caveolin-1 expression is a predictor of recurrence-free survival in pT_2N_0 prostate carcinoma diagnosed in Japanese patients. Cancer 2003;97:1225–33.
16. Wu C, Butz S, Ying Y, Anderson RG. Tyrosine kinase receptors concentrated in caveolae-like domains from neuronal plasma membrane. J Biol Chem 1997;272:3554–9.
17. Vey M, Pilkuhn S, Wille H, et al. Subcellular colocalization of the cellular and scrapie prion proteins in caveolae-like membranous domains. Proc Natl Acad Sci U S A 1996;93:14945–9.
18. Bilderback TR, Gazula VR, Lisanti MP, Dobrowsky RT. Caveolin interacts with Trk A and p75(NTR) and regulates neurotrophin signaling pathways. J Biol Chem 1999;274:257–63.
19. Pflug B, Djakiew D. Expression of p75NTR in a human prostate epithelial tumor cell line reduces nerve growth factor-induced cell growth by activation of programmed cell death. Mol Carcinog 1998;23:106–14.

Downloaded from http://aacrjournals.org/cancerres/article-pdf/66/10/5159/2550770/5159.pdf by guest on 11 February 2025